Modeling Starburst Cells' $GABA_B$ Receptors and Their Putative Role in Motion Sensitivity

Norberto M. Grzywacz* and Charles L. Zucker†
*Department of Biomedical Engineering, Neuroscience Graduate Program, and Center For Visual Science and Technology, University of Southern California, Los Angeles, California; and †Department of Anatomy and Neurobiology, Boston University School of Medicine, Boston, Massachusetts

ABSTRACT Neal and Cunningham (Neal, M. J., and J. R. Cunningham. 1995. *J. Physiol. (Lond.)*. 482:363–372) showed that $GABA_B$ agonists and glycinergic antagonists enhance the light-evoked release of retinal acetylcholine. They proposed that glycinergic cells inhibit the cholinergic Starburst amacrine cells and are in turn inhibited by GABA through $GABA_B$ receptors. However, as recently shown, glycinergic cells do not appear to have $GABA_B$ receptors. In contrast, the Starburst amacrine cell has $GABA_B$ receptors in a subpopulation of its varicosities. We thus propose an alternate model in which $GABA_B$-receptor activation reduces the release of ACh from some dendritic compartments onto a glycinergic cell, which then feeds back and inhibits the Starburst cell. In this model, the GABA necessary to make these receptors active comes from the Starburst cell itself, making them autoreceptors. Computer simulations of this model show that it accounts quantitatively for the Neal and Cunningham data. We also argue that $GABA_B$ receptors could work to increase the sensitivity to motion over other stimuli.

INTRODUCTION

One of the most important unanswered questions in retinal neurobiology is why the Starburst cholinergic amacrine cells have two neurotransmitters (1–4). These cells produce both acetylcholine (ACh) and γ-aminobutyric acid (GABA), releasing them upon light stimulation (5–9). The released ACh has many roles in the retina, including the enhancement of motion sensitivity (10–12) and the establishment of directional selectivity for some types of stimuli (13–20). In turn, recent evidence shows that GABA is the main transmitter involved in directional selectivity (6,7,21). In this article, we discuss another possible role suggested by the cholinergic amacrine cells themselves containing $GABA_B$ receptors (22). Because these receptors often work as autoreceptors in the brain (23–25), this raises the possibility that GABA from these cells feeds back onto them to control their release of ACh. This control could be by hyperpolarization (26,27), by reducing a Ca^{2+}-dependent current (28–30) through a G-protein mechanism (30–32), or by facilitating a L-type Ca^{2+} channel (33). The results of Neal and Cunningham (5) coupled to the results of Zucker et al. (22) lend some support to such an autoreceptor control (see also (34)). Neal and Cunningham showed that the $GABA_B$ agonist baclofen and the glycinergic antagonist strychnine enhance the light-evoked release of retinal ACh. Considering these results, they proposed that glycinergic cells inhibit the Starburst cells and are in turn inhibited by GABA through $GABA_B$ receptors. However, as shown by Zucker et al. (22), glycinergic cells do not appear to have $GABA_B$ receptors. Consequently, one must search an alternate hypothesis for the role of these receptors. The simplest alternative given the available data is that $GABA_B$ agonists enhance the release of ACh by acting on the Starburst cells themselves. These cells may synapse onto glycinergic cells (which probably include the cholinoreceptive DAPI-3 cell (22,35,36) through muscarinic receptors. (The receptors may be chemically ephaptic, that is, ACh may diffuse to targets far from the presynaptic site; this would help to explain the apparent dearth of conventional synapses made by Starburst cells onto noncholinergic amacrine cells (37)). In addition, retinal cholinergic receptors are often far away from the site of cholinergic release (38)—the glycinergic cells of ACh may provide contact back onto Starburst cells (5,39). Hence, the activation of $GABA_B$ receptors may result in disinhibition.

In this article, we use a biophysical model to test the feasibility of the $GABA_B$-autoreceptor hypothesis for Starburst cells. To know whether this hypothesis will work is not so easy. One difficulty is to know how $GABA_B$ agonists reduce the muscarinic input to the glycinergic cell at the same time that they increase the overall release of ACh. Perhaps the answer lies in the recent surprising finding that only ~25% of Starburst-cell varicosities contain $GABA_B$ receptors (22). If the input to glycinergic cells came only from these varicosities, then $GABA_B$ agonists might affect these cells without reducing ACh release from other varicosities. However, the model must solve another problem with GABAergic action on Starburst cells. The release of ACh from Starburst cells may be also inhibited by GABA through $GABA_A$ receptors (8,16,39,40). How is it that the GABA that putatively feeds back to the $GABA_B$ autoreceptor does not inhibit the ACh release through the $GABA_A$ heteroreceptor? The model provides answers to these questions and fits the Neal and Cunningham data well. An abstract version of the model appeared elsewhere (41).

Submitted August 8, 2005, and accepted for publication April 10, 2006.

Address reprint requests to Norberto M. Grzywacz, Tel.: 213-821-1150; E-mail: nmg@bmsr.usc.edu.

0006-3495/06/07/473/14 $2.00

doi: 10.1529/biophysj.105.072256

The next section of this article will provide the model assumptions and their justifications, along with a physical description of the model. That section will include no equations to facilitate the comprehension of the ideas. The model equations and the parameters used in the simulations will appear in Appendices A and B, respectively.

MODEL

Fig. 1 shows the architecture of the model. We do not intend it to capture all the known details of the cells. Rather, we want it to be the simplest model that accounts for the Neal and Cunningham article (5) and be generally consistent with the knowledge in the field. To start, the model simulations used only the ON-pathway (42–45), assuming the OFF-pathway to be similar. Moreover, all model cells except for the Starburst cell had just one compartment. In turn, the Starburst cell had five compartments, a soma, and two proximal and two distal dendritic compartments. The reason for having two of each of these compartments was to enforce morphological symmetry about the soma (44,46).

The reason for having proximal and distal dendritic compartments in the model was to segregate $GABA_A$ and $GABA_B$ receptors. Both these receptors are present in Starburst cells (8,16,22,39,40), but it is necessary to allow for the GABA acting on $GABA_B$ receptors not to act on $GABA_A$ receptors. If such simultaneous actions were to occur, then the cell would be shut down by its own GABA. One can conceive other mechanisms for preventing such simultaneous actions that do not invoke spatial segregation of receptors. For instance, $GABA_A$ receptors could be sensitive to GABA at a different range of concentrations than $GABA_B$ receptors. Nevertheless, the assumption of receptor segregation receives support by the compartmentalization of $GABA_B$ receptors in ~25% of Starburst-cell varicosities (22). Hence, the relative amount of $GABA_A$ and $GABA_B$ receptors is likely to vary across varicosities. Segregation of GABAergic receptors into different portions of the dendrites is similar to that proposed for Cl^- cotransporters in Starburst cells (21). Furthermore, the inhomogeneity of the $GABA_B$ receptors also resembles that of Kv3 K^+ channels in Starburst cells (47). However, we attach no significance to the proximal versus distal inhomogeneity in the model. No direct evidence is available for such inhomogeneity, but this may not be important. We only assume it here for simplicity and simulations with an inverted disposition of $GABA_A$ and $GABA_B$ receptors yield similar results to those in this article.

Because $GABA_B$ receptors are proximal in the model, the synapse to the glycinergic cell must also be proximal. From the data of Neal and Cunningham (5) and Zucker et al. (22), we assume that this synapse is muscarinic. (One could also use nicotinic and $GABA_A$ synapses, but this would make the

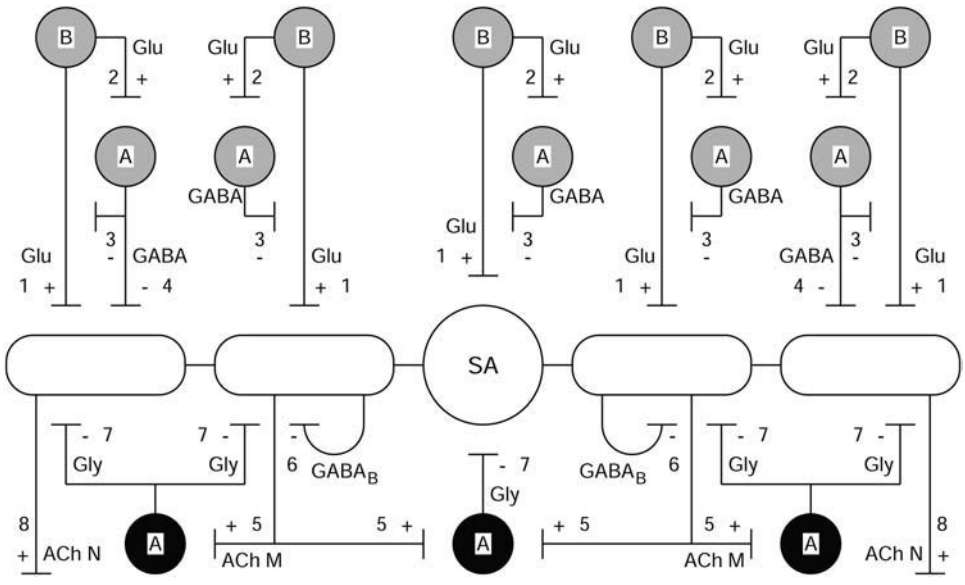

FIGURE 1 New model for the function of $GABA_B$ receptors in the control of retinal cholinergic release. In this figure, circles, and rounded rectangles represent somas and dendrites, respectively. The *T* terminations represent synapses onto somas and onto dendrites, with the plus symbol (+) indicating excitatory synapses and the minus symbol (−) indicating inhibitory synapses. The main cell in the model is the Starburst cell, whose soma is labeled *SA* and which, for simplicity, contains four dendritic compartments. Other cells include the bipolar cells (labeled *B*) and two types of amacrine cells (labeled *A*), one GABAergic and one glycinergic (labeled *Gly*). The direct pathway to the Starburst cell appears textured, whereas the inhibitory feedback pathway appears in black. Bipolar cells making glutamatergic synapses (labeled *Glu*) are the beginning of the excitatory pathway. They feed the Starburst cell (synapses labeled *1*) and the GABAergic cells (synapses labeled *2*). In turn, the GABAergic cells feed the bipolar inputs (synapses labeled *3*) and the distal dendrites of the Starburst cells (synapses labeled *4*). The proximal dendrites release ACh, which excites the glycinergic cell through muscarinic receptors (labeled *ACh M* and synapses labeled *5*). This ACh release that activates muscarinic receptors is controlled by GABA, which is released from the proximal dendrite and feeds back to it through $GABA_B$ receptors (synapses labeled *6*). Activation of the muscarinic receptors on the glycinergic cell causes it to inhibit the Starburst cell (synapses labeled *7*). As a result, there is a reduction of cholinergic release from its distal dendrites. (These dendrites normally feed ganglion cells through nicotinic receptors—labeled *ACh N* and synapses labeled *8*.) If the distal cholinergic release is much larger than the proximal one, then the model can account for the results of Neal and Cunningham (5). (Evidence suggests that different dendritic varicosities of the Starburst cell may have different relative amounts of $GABA_A$ and $GABA_B$ receptors (see Model, in text, for arguments. The division into proximal and distal dendritic compartments is only for simulation simplicity.)

model unnecessarily complex.) Furthermore, it is postulated that GABA is released in a Ca^{2+}-independent manner (48–50) by the proximal dendritic compartment and feeds back onto it. This assumption is not completely realistic, because some GABA release from Starburst cells is Ca^{2+} dependent (51). However, in varicosities with $GABA_B$ receptors, their action suppresses Ca^{2+}-dependent release of GABA. Consequently, such a release would only occur early in the response, that is, before $GABA_B$ action begins. Because the stimulus' period (333 ms; see Appendix B) is much slower than most synapses, any Ca^{2+}-dependent release would occur during a negligible portion of the response in the proximal compartment of the model. Nevertheless, such a release could happen in the distal compartment, making the model still compatible with the data of Zheng et al. (51). Thus, for simplicity, we only included Ca^{2+}-independent release of GABA in the proximal compartment.

The activation of the $GABA_B$ autoreceptor would reduce the gain of the muscarinic synapse by lowering the influx of Ca^{2+} into the presynaptic site (28–30). Hence, the glycinergic cell and its synapse would be less active and thus inhibit less the Starburst cell (Fig. 1). (Alternatively, the glycinergic cell could inhibit the bipolar-cell input onto the Starburst amacrine cell (37).) This disinhibition would increase the release of ACh. How is it possible for the ACh release to increase at the same time that the muscarinic synapse is becoming weaker? Again, since $GABA_B$ receptors exist only proximally in the model, one can answer this question if one postulates that there is distal cholinergic release. What one needs is for the distal release to dominate the overall release. Therefore, even though the ACh release that activates muscarinic receptors falls, the total release may increase. Fortunately, there is evidence that Starburst dendrites normally release ACh onto ganglion-cells' nicotinic receptors (7,52–56).

Bipolar cells making glutamatergic synapses are the beginning of the model's excitatory pathway. These cells receive the visual input (not shown in Fig. 1), and synapse onto the Starburst and the GABAergic amacrine cells. In turn, the GABAergic cells feed the bipolar inputs and the distal dendrites of the Starburst cells. There is evidence for a GABAergic feedback onto the bipolar cells feeding the Starburst cell (57). The GABAergic synapse onto the bipolar cells could be through $GABA_A$ (58–61) or $GABA_C$ (59,62–64) receptors. In this article, we will assume for simplicity that the GABAergic synapses onto bipolar and distal Starburst dendrites are identical.

METHODS

With one exception, the simulations of the model included only one type of stimulus: a full-field square-wave stimulation whose definition and parameters appear in the Appendices. (The exception appears in the Discussion and we describe it there.) The computer simulated the response by solving numerically the system of differential equations representing the model (Appendix A). This solution used the Dormand-Prince method with adaptive step size (65) and was implemented in MatLab using Simulink (The MathWorks, Natick, MA).

All the solutions of the equations used the same parameters, which appear in Appendix B. With one exception (explained below), we did not attempt to optimize parameters finely, but only to capture the data qualitatively. Several parameters were around values estimated from the literature. We used parameters as close as possible to the cells of interest, but sometimes, the only ones we could find were not even for the retina. We used them anyway, as they at least constrained our simulations to realistic values.

Parameters estimated from the literature were as follows: We used a specific membrane-capacitance value of 1 $\mu F/cm^2$. This was close to the value measured for bipolar, amacrine, and ganglion cells of mudpuppy and tiger-salamander retinas (66). In turn, for membrane time constants, we used characteristic vertebrate-neuron values of 10–20 ms (but see (66)). These values came, for example, from the Guinea-pig's hippocampal neurons (67), and from the cat's spinal motoneurons (68) and sensory-motor-cortex cells (69). Values for resting potentials were -50 mV, as recorded in the turtle's amacrine cells (70). Amacrine-cell soma diameters were between 5 and 10 μm, as in the cat's AII amacrine cells (71), the primate's Starburst amacrine cells (72), and the pigeon's amacrine cells (73). $GABA_A$ and glycinergic reversal potentials were typical for the retina by being between -60 and -50 mV. For instance, studies on $GABA_A$ and glycinergic synapses were performed respectively with the turtle's cone photoreceptors (74) and the tiger salamander's amacrine cells (75). In turn, muscarinic receptors reversed at $\sim$0 mV in most vertebrate tissues. The information on these receptors came, for example, from the bullfrog's sympathetic ganglia (76), the Guinea-pig's smooth muscles (77), and the bovine ciliary muscle cells (78). Finally, we set glutamatergic receptors to reverse at 20 mV, as for the Guinea-pig's laterodorsal tegmental neurons (79).

Different from these parameters, we had no good experimental basis to select other synaptic parameters. For instance, maximal synaptic conductances for our simulations would depend on light-stimulus properties, such as intensity. Such conductances had not been measured in conditions similar to those that we were trying to simulate. Hence, we selected these conductances based on the resting conductances of the membrane. The maximal glutamatergic conductance was the same as the resting conductance of the cellular compartments. Our rationale was that much smaller glutamatergic conductances would depolarize the cell too little, whereas much larger ones would saturate it. Similar considerations were used for the muscarinic conductance. In contrast, the glycinergic conductance was four times stronger than the resting conductance to produce shunting inhibition (with a similar rationale applying to the $GABA_A$ synapse). We tested the robustness of our results with these conductance choices by varying each of them individually by 25% up or down. Our fits remained inside the range of the experimental values (Figs. 6 and 8) despite these variations.

We only explored the parameter space systematically for slopes and thresholds of the synapses' input-output relationships (Eq. A2 in Appendix A). The exploration was such to ensure that all modeling fits stayed inside the experimental range (Figs. 6 and 8). Furthermore, best parameters were those that brought fits as close as possible to the middle of it. For all synapses, except the nicotinic one, we searched for threshold parameters coarsely, beginning at -50 mV (the cells' resting potential). We moved them up and down in units of 10 mV. We also searched for slopes coarsely, starting at 1 mV^{-1} and moving in units of 0.5 mV^{-1}. The only parameters for which we made an effort to optimize finely were those of the nicotinic synapse. This was because it is the main process determining cholinergic release, the output of the Neal and Cunningham experiments. To optimize the parameters controlling this release, we fixed all other parameters at their coarse optimal values and used a Nelder-Mead simplex (direct search) method (80). After optimization, we tested the robustness of our results by varying slopes and thresholds individually. Slopes and thresholds were varied up or down by 0.25 mV^{-1} and 0.5 mV, respectively. The only exception was the nicotinic slope, which we vary up and down by 0.1 mV^{-1}

(almost a third of the final value). Again, our fits remained inside the range of the experimental values (Figs. 6 and 8) despite these variations.

RESULTS

The simulations in this section are organized according to the experimental conditions used, first considering the control condition, and then the effects of baclofen, strychnine, and bicuculline.

Control

The first things to consider, in understanding the model's behavior, are the potentials in control conditions in the various compartments. The most-central compartments for this understanding are those of the Starburst amacrine cell. In Fig. 2, we show the potentials in this cell's soma and distal dendritic compartment (Fig. 1) in response to a full-field square-wave modulation. Appropriately, the response is periodic. As seen in Fig. 2 *A*, the response reaches equilibrium essentially during the first cycle. Fig. 2 *B* shows the voltage's details in one of the cycles. Not surprisingly, there is much voltage attenuation from the distal dendrite to the soma. In addition, the voltage waveforms are complex, showing two peaks during the cycle. The reason for these peaks will be understood when we consider the glycinergic input to the Starburst cell.

From these potentials it is not difficult to understand how ACh is released. Fig. 3 shows the release from the distal dendritic compartment (labeled *nicotinic* in Fig. 3) and from the proximal dendritic compartment (labeled *muscarinic* in Fig. 3) during one cycle of the response. One can see that the ACh release that activates nicotinic receptors follows the potential in the distal dendritic compartment of the Starburst cell. Both this release and the potential have two simultaneous peaks. In contrast, the ACh release that activates muscarinic receptors has only one peak, which temporally coincides with the first peak of the ACh release that activates nicotinic receptors. The disappearance of the second muscarinic peak is due to the activation of the $GABA_B$ autoreceptors, which is local to the proximal dendritic compartment (Fig. 1). As also seen in Fig. 3, the ACh release that activates nicotinic receptors is much larger than the ACh release that activates muscarinic receptors. Consequently, the overall cholinergic release in the model is dominated by the ACh release that activates nicotinic receptors. This domination allows us to explain how ACh release that activates muscarinic receptors can fall under baclofen at the same time that the total release increases (see Model).

Baclofen

The most important drug used by Neal and Cunningham was baclofen, an agonist of $GABA_B$ receptors; Fig. 4 illustrates its effects on key potentials and synaptic releases. Inspection of

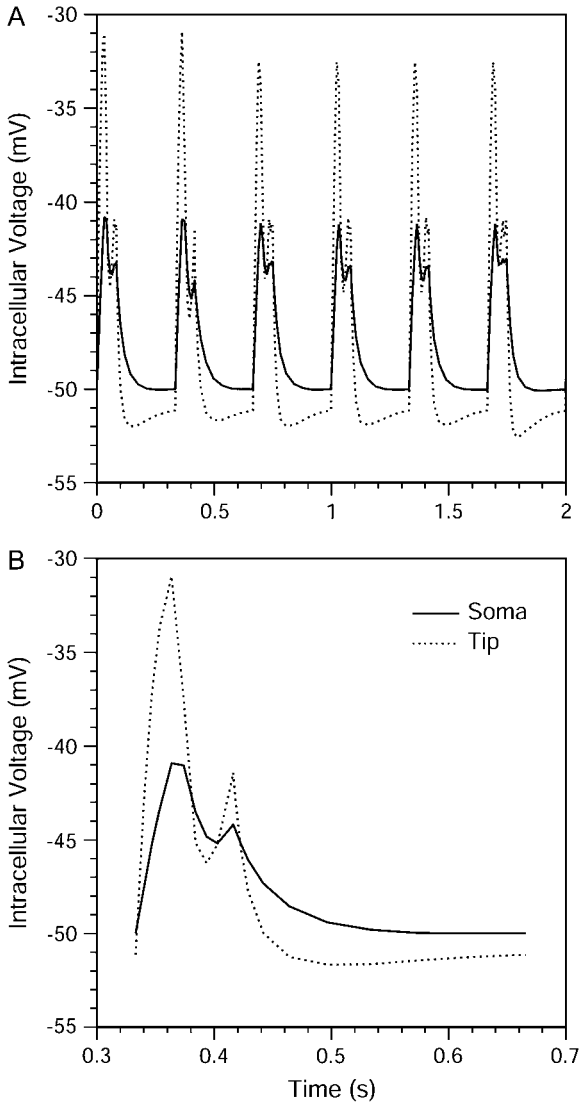

FIGURE 2 Somatic and dendritic voltages of the model's Starburst cell in control condition. The recorded dendrite is the distal one (*top*) in Fig. 1. The stimulus giving rise to these recordings is a 3 Hz full-field square-wave modulation over 2 s with 25% duty-cycle. As seen in panel *A*, model cells reach equilibrium essentially during the first cycle. Panel *B* is for the second cycle of the top graph, but with an expanded timescale. One can see that the depolarization is attenuated from the dendrite to the soma and that the waveforms are complex, having two peaks during the cycle.

Fig. 4, *A* and *B*, shows that the first peak of potential in the Starburst cell causes simultaneous muscarinic and autoreceptor-GABAergic release. (Fig. 4 *B* shows that the autoreceptor-GABAergic activation produces a small dip in the ACh release that activates muscarinic receptors.) Because of the ACh release that activates muscarinic receptors, the glycinergic cell responds, albeit with some delay (Fig. 4 *A*). The feedback of the glycinergic cell onto the Starburst cell then causes the complex waveform of the Starburst cell's response. The peak of the glycinergic potential coincides with the valley in the Starburst response, showing that this valley is

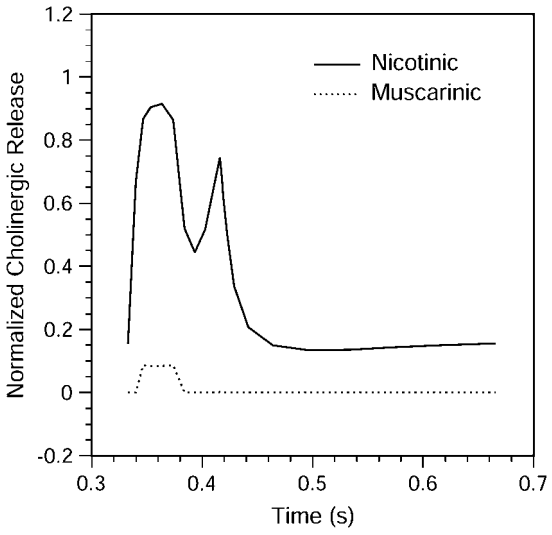

FIGURE 3 Cholinergic release in control condition in the model. The release is shown for the synapses *5* (here labeled *muscarinic*) and *8* (here labeled *nicotinic*) of Fig. 1. We are normalizing the individual releases by the maximum of their sum and the period of the release is the same as in Fig. 2 *B*. The ACh release that activates nicotinic receptors is much larger than its muscarinic counterpart. The nonzero release between 0.46 and 0.66 s reflects the tonic cholinergic release without light stimuli.

due to the glycinergic feedback. As the glycinergic activity falls, the Starburst potential rises again, generating the second peak. This peak is smaller than the first peak because of the glycinergic inhibition. This peak's smallness, coupled to the autoreceptor inhibition, essentially prevents further ACh release that activates muscarinic receptors. When one adds baclofen (Fig. 4, *C* and *D*), dramatic effects occur both in the potentials and in the transmitter releases. Baclofen boosts the $GABA_B$ activity so much that all ACh release that activates muscarinic receptors is canceled (Fig. 4 *D*). As a result of this cancellation, the glycinergic potential does not rise, causing the Starburst potential to be larger and unimodal (Fig. 4 *C*).

Strychnine

In many respects, strychnine, a glycinergic antagonist, mimics the effects of baclofen, because both drugs reduce the output of the glycinergic synapse. Fig. 5 illustrates the similarity of the effects. Fig. 5 *A* of this figure is identical to that in Fig. 4 *A*, but Fig. 5 *B* shows total cholinergic release instead of just ACh release that activates muscarinic receptors. Not surprisingly, both cholinergic and glycinergic releases follow the potentials at the Starburst and glycinergic cells, respectively. When one adds strychnine (Fig. 5, *C* and *D*), the cholinergic release (Fig. 5 *D*) becomes more potent and longer lasting (the two peaks merge). This is because there is no glycinergic inhibition of the cholinergic cell. Curiously though, this does not mean that glycinergic release is over and inspection of Fig. 5 *D* shows that this release is also boosted. What is absent is the activation of glycinergic receptors on the Starburst cell. Because of the lack of this activation, the Starburst potential is larger and longer (Fig. 5 *C*), causing more ACh release that activates muscarinic receptors and thus, larger glycinergic potential (Fig. 5 *C*).

These results with baclofen and strychnine are consistent with Neal and Cunningham's Figs. 1–3 and their Fig. 5. Moreover, the muscarinic control of glycinergic release in the model is consistent with their Fig. 6. As our Fig. 6 shows, although the model is simplistic in details, it fits these data quantitatively (*first four columns* in our Fig. 6). These fits include data on background as well as light-evoked release of ACh. And the model also fits the data when one combines baclofen and strychnine (*fifth column* in our Fig. 6). Using this combination of drugs yields the same increase in cholinergic release as when each drug is used in isolation (*second* and *fourth columns*). This should not be surprising, as the main effect of both these drugs is to kill glycinergic action on the Starburst cell.

Bicuculline

Neal and Cunningham also used bicuculline, a $GABA_A$ antagonist, in addition to baclofen and strychnine. Fig. 7 shows how the model reacts to bicuculline and to its combination with baclofen. Bicuculline causes a relatively small increase in the Starburst potential without eliminating its two peaks (Fig. 7 *A*). This increase follows an increase in the bipolar input to the Starburst cell. Furthermore, the increase in Starburst potential follows a reduction of the inhibition in this cell's distal dendritic compartment (Fig. 1). As a result of this increase in potential, the cholinergic release also undergoes a small augmentation (Fig. 7 *B*). The increase in potential is much more dramatic when one adds baclofen to the bicuculline (Fig. 7 *A*). Comparison of Figs. 4 and 7 reveals that the combination of bicuculline and baclofen causes a larger increase in potential than with each drug in isolation. This dramatically increased potential leads to a boosted release of ACh (though the boost seems to be in the duration of the release and not in its total amplitude).

As for baclofen and strychnine, the results with bicuculline are also consistent with Neal and Cunningham's data (see their Fig. 4). And the model again provides a quantitatively good fit to the data as shown in our Fig. 8. The fit applies to bicuculline's effect on background and on light-evoked release of ACh. In addition, the fit applies to the simultaneous effect of bicuculline and baclofen.

DISCUSSION

We model the circuit linking Starburst and glycinergic amacrine cells, and account for a host of pharmacological conditions (5). The model postulates that $GABA_B$ receptors on the Starburst cell function as autoreceptors, whose role is to control the cholinergic contact onto glycinergic cells. In turn, these cells feed-back onto the Starburst cell, inhibiting it with glycine. This feedback loop is sufficient to account quantitatively

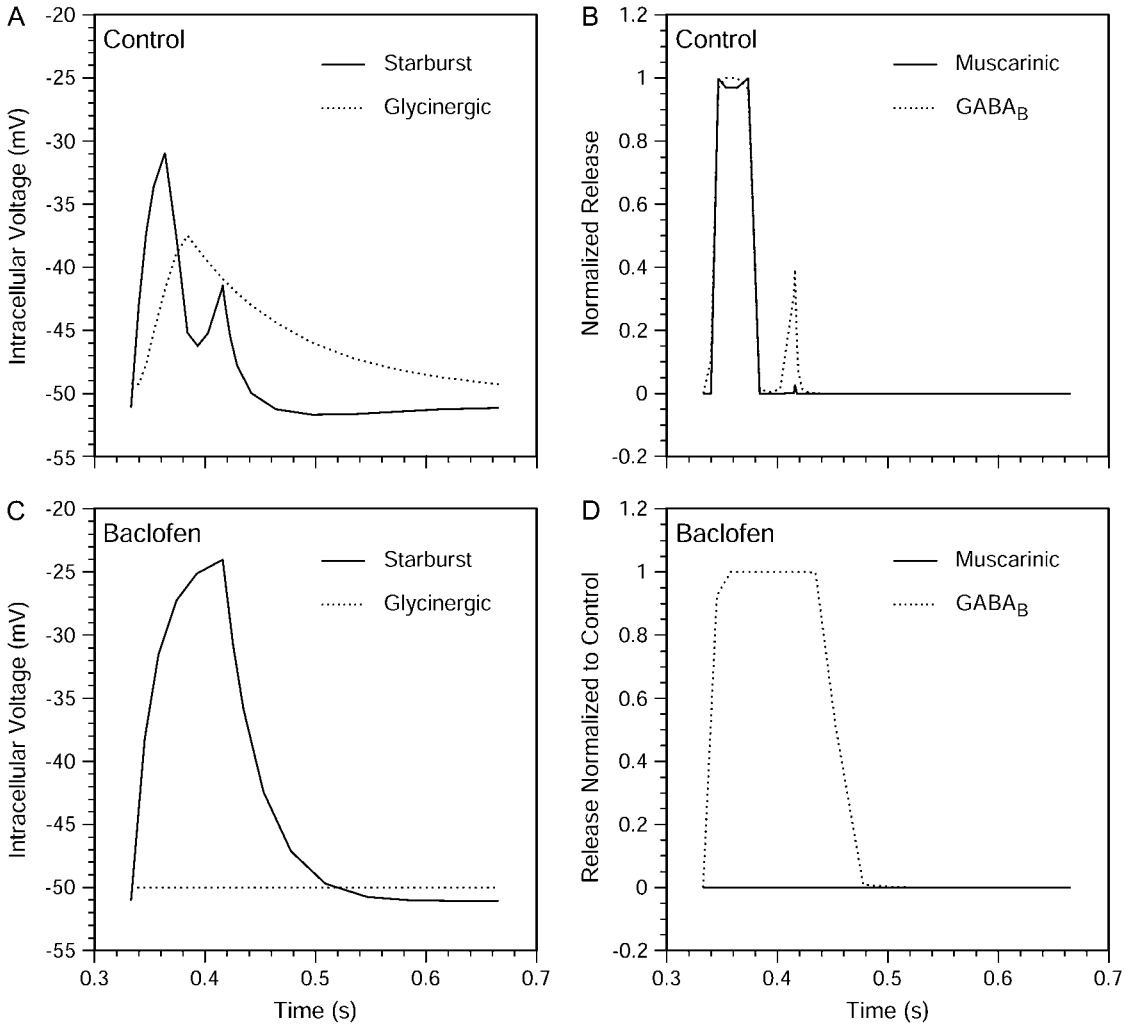

FIGURE 4 Effect of baclofen in the model. This effect is shown for the voltages at the glycinergic cell and at the distal dendrite of the Starburst cell (*A* and *C*). Moreover, the figure displays the effect for transmitter release at the Starburst cell's muscarinic (synapses labeled *5* in Fig. 1) and $GABA_B$ (synapses labeled *6* in Fig. 1) synapses (*B* and *D*). We show these voltages and releases over the same period as in Fig. 2 *B*. At each synapse, the plots normalize release to the maximum release in control condition. Panel *A* shows that the two control-voltage peaks result from the rise of glycinergic activity exactly at the minimum between the peaks. Baclofen eliminates the glycinergic activity, destroying the two peaks and increasing depolarization in the Starburst cell (*C*). This elimination of glycinergic activity is due to the blockade of ACh release that activates muscarinic receptors by baclofen (*D*). Baclofen's induced increase in depolarization causes several processes to increase in amplitude, including the release at the $GABA_B$ synapse. This synapse's role can be appreciated in control conditions when its maximal release coincides with a small local minimum at the ACh release that activates muscarinic receptors (*B*).

for the increased release of ACh under baclofen and strychnine (Figs. 4–6). Moreover, this loop can explain the reduced glycinergic release by baclofen (Fig. 4) and the effect of muscarinic drugs on this release (Fig. 1). Effects involving $GABA_A$ antagonists are accounted for, too (Figs. 7 and 8).

Limitations of the model

The main limitations of the model are due to the simplicity of its components. Perhaps its main simplifying feature is its segregation of GABAergic receptors, and of ACh release that activates nicotinic and muscarinic receptors into different dendritic compartments of the Starburst cell. We already discussed the rationale and limitations of this segregation assumption in Model. In Experimental Predictions, we will address some of the consequences of segregation.

To make the model more realistic, one would have to include better morphological structure for all cells (Fig. 1). In addition, one would have to use synaptic mechanisms and inputs to bipolar cells that are more realistic (Appendix A). A benefit of using realistic morphology for the Starburst cell would have been an assessment of the spatial-separation requirements for this cell's synaptic inputs and outputs. The details of this cell's response dynamics would also change, but we do not believe that the main conclusions would be modified (Model). The synapses are modeled without dynamics—that is, assuming that they are sufficiently fast to be in quasi steady state. This is probably true, since the

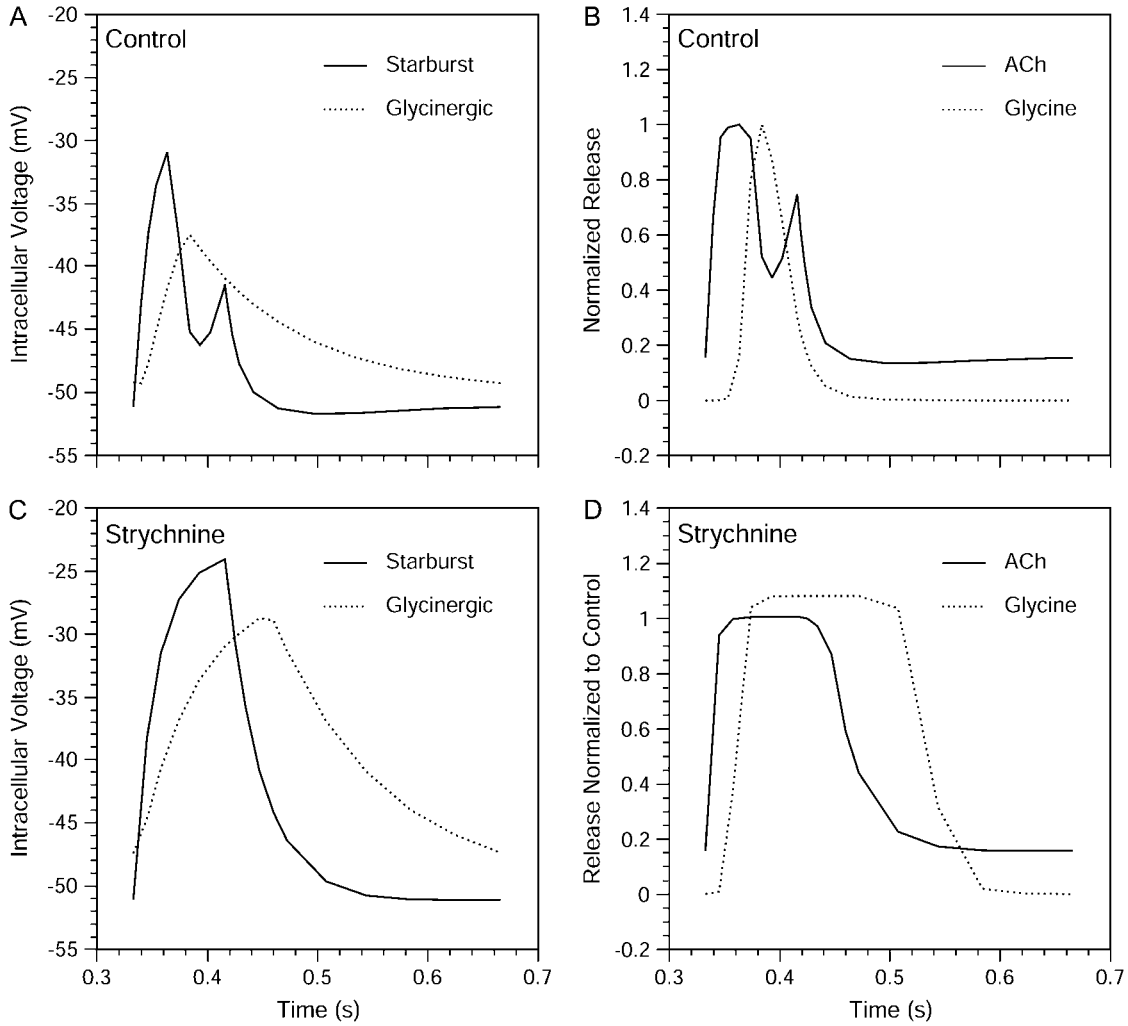

FIGURE 5 Effect of strychnine in the model. This effect is shown for the same variables as in Fig. 4, except that the releases are of ACh (sum of synapses labeled *5* and *8* in Fig. 1) and glycine (synapses labeled *7* in Fig. 1). (*A–D*) Plotting conventions, and periods are also as in Fig. 4. This figure confirms and extends the conclusion of Fig. 4 that the two control-voltage peaks result from the rise of glycinergic activity exactly at the minimum between the peaks (*A*). Strychnine does not eliminate glycinergic release (*D*), but eliminates its postsynaptic action. As a result, strychnine destroys the two peaks and increases the depolarization in the Starburst and glycinergic cells (*C*). Therefore, ACh and glycine releases also increase (*B* and *D*).

stimulus' period (333 ms; see Appendix B) is much slower than most synapses. However, this may not apply to the $GABA_B$ synapse, since it may depend on a G-Protein second-messenger pathway (30–32). If we were to slow down this synapse in the model, the dynamics of the responses would change and the autoreceptor control may lose its effectiveness at high temporal frequencies. The stimulus' slowness is also our justification for disregarding the dynamics of the input to the bipolar cell (Appendix A). However, it would have been better not to neglect these dynamics if we wanted to predict the results of faster experiments. Moreover, the model input to the bipolar cell neglected surround-inhibition from horizontal cells. This hampers the ability to make predictions on the effect of spatial frequency. If spatial frequency were of interest, then one would have to include a richer spatial representation of the inputs. Because the stimuli are full-field square-waves (Methods), there is no need to worry about spatial frequency. For these stimuli, surround-inhibition only reduces the bipolar-cell gain.

Functional roles

The roles of several components of the model have been discussed elsewhere. For instance, the role of the GABAergic input to the bipolar cells may be to give the retina a degree of transience (81–83). In turn, one role of the GABAergic input to the distal dendrites of the Starburst cell may be to contribute to directional selectivity ((16,84); but see (85)). What could be the role of the $GABA_B$-controlled glycinergic feedback loop to the Starburst cell? We propose that this loop could work to make the sensitivity of ACh release in response to motion larger than those in response to other stimuli. Acetylcholine has been proposed to be involved in the enhancement of retinal motion sensitivity

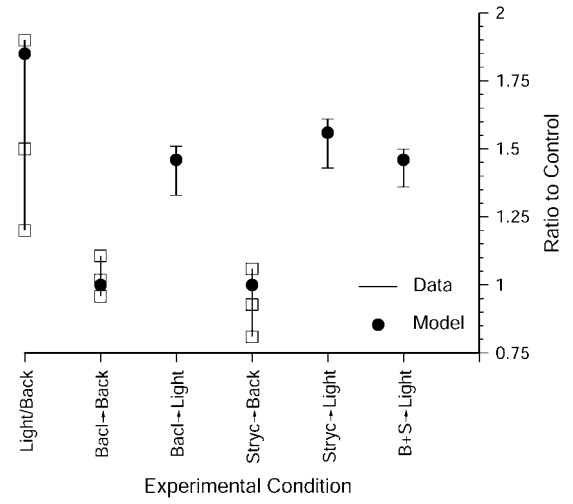

FIGURE 6 Comparison between experiments and model on the effects of baclofen and strychnine. The experimental data are total ACh releases taken from Neal and Cunningham (5). These data appear either as standard-error bars (if provided by the authors), or as ranges (given by the *lower* and *higher white squares*) and medians (given by the *middle square*). The categories in the data's horizontal axes are as follows: *Light/Back* is the ratio between light-evoked and spontaneous releases in control condition. *Bacl → Back* and *Stryc → Back* are the post- to pre-drug ratios of spontaneous release for baclofen and strychnine, respectively. *Bacl → Light* and *Stryc → Light* are the post- to pre-drug ratios of light-evoked release for baclofen and strychnine, respectively. *B+S → Light* is the same, but for using baclofen and strychnine simultaneously. The model values fall within the experimental ranges and error estimates for all control, baclofen, and strychnine conditions.

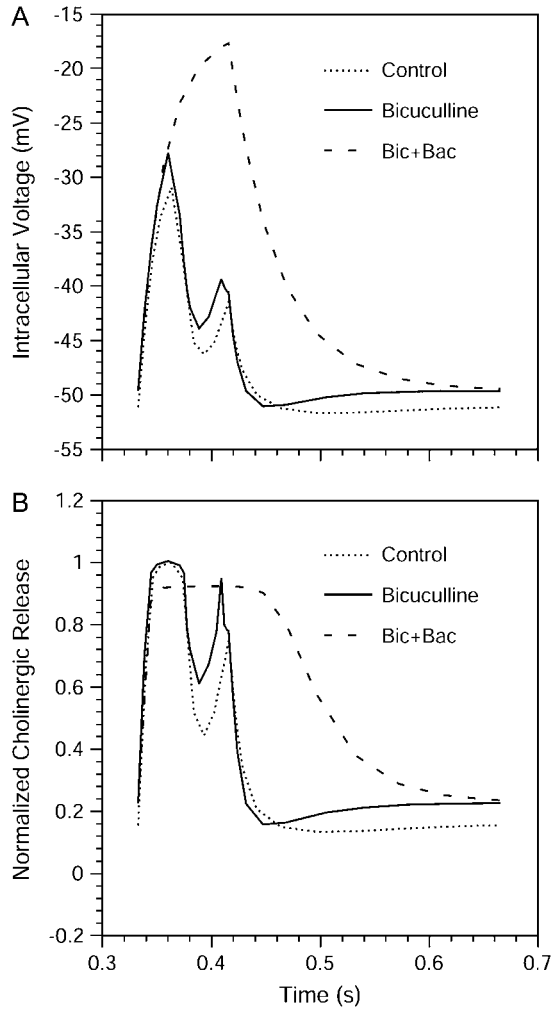

FIGURE 7 Effect of bicuculline and baclofen in the model. To illustrate this effect, we use the voltage at the distal dendrite of the Starburst cell (*A*). Furthermore, the figure displays the effect for cholinergic release from this cell (sum of Synapses 5 and 8 in Fig. 1). (*B*) The display conventions and periods are as in Fig. 4. In this figure, the curve *Bic+Bac* corresponds to the condition where bicuculline and baclofen are both applied. Bicuculline increases the depolarization of the Starburst cell and thus the cholinergic release. Adding baclofen to bicuculline causes further depolarization and cholinergic release, though the latter rises mostly due to the prolongation of the response.

(10–12) and in preferred-direction facilitation in directionally selective cells (10,86,87). Here is how we think of the $GABA_B$-receptor involvement in these motion functions. If one suddenly delivers a no-motion stimulus to the Starburst cell, then the $GABA_B$ action on the muscarinic synapse may not have time to react. This is because a slow G-protein second-messenger system may mediate this action (30–32). Without this action, muscarinic activation of the glycinergic cell can occur and thus, there is inhibitory feedback onto the Starburst cell (Fig. 1). If instead of sudden stimuli, a sufficiently slow motion sweeps through the Starburst cell, then a different set of events take place. Consider a motion sweeping from left to right in Fig. 1. The left bipolar cells will be the first to be made active, depolarizing the Starburst cell. This depolarization would start the $GABA_B$ loops (synapses labeled *6* in Fig. 1) even before the motion reaches the right bipolar cells. In this case, when the motion finally reaches them, the ACh release that activates muscarinic receptors to the glycinergic cell is truncated, eliminating the glycinergic feedback onto the Starburst cell.

To illustrate these predictions of the model, we added an artificial constant delay to the $GABA_B$ synapse (Eq. A4 in Appendix A). Furthermore, we activated the bipolar cells sequentially to simulate motion. These cells were still activated by a 3-Hz square-wave (Eq. A1). However, the cycle of any given bipolar cell started after that of the neighbor to its left by a preset delay. For example, in Fig. 9 *A*, this delay was 100 ms, implying an edge motion sweeping the Starburst cell in 400 ms from left to right. The figure shows the response as recorded on the right distal dendritic compartment. As predicted, the response to the motion was larger than the response to the full-field stimulation (Fig. 9 *A*). With this delay and this motion, the facilitation of the amplitude of response above resting potential was 84.1%. Without the $GABA_B$ delay, facilitation disappeared (only 7.6% for this motion and negative for other motions). However, although the $GABA_B$ delay had effects on the details of the responses, it did not affect the qualitative effects of the various pharmacological drugs described earlier in the article. Even

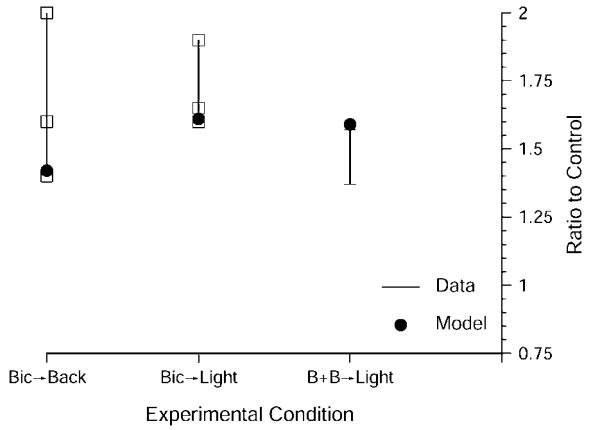

FIGURE 8 Comparison between experiments and model on the effects of bicuculline and baclofen. The data's source and figure's conventions are as in Fig. 6. The categories in the data's horizontal axes are as follows: *Bic → Back* and *Bic → Light* are the post- to pre-drug ratios of spontaneous and light-evoked releases, respectively, for bicuculline. $B + B \rightarrow Light$ is the post- to pre-drug ratio of light-evoked releases for baclofen starting from a bicuculline condition. Again, the model values fall within the experimental ranges and error estimates for all bicuculline and baclofen conditions.

with this delay, baclofen and strychnine still increased the response (compare Fig. 9 *B* with the *solid line* of Fig. 9 *A*). Bicuculline alone did not have a major effect on the response (compare Fig. 9, *A* and *B*). But bicuculline augmented the effect of baclofen (Fig. 9 *B*). These results with baclofen, strychnine, and bicuculline were similar to those in Figs. 4–8.

Hence, the model predicts that the Starburst cell's responses and release of ACh may be larger for motion than for other stimuli. In the example above, the enhancement of the responses to motion is particularly relevant for the right dendrites. This is because the left dendrites may be inhibited by $GABA_A$ mechanisms. If the right dendrites make preferential synapses onto directionally selective cells with rightward preferred-direction (16,17), then $GABA_B$ receptors may be crucial for preferred-direction facilitation in these cells. The same would hold for directionally selective cells with different preferred directions.

Experimental predictions

One novel aspect of the model is the proposal that $GABA_B$ receptors work as autoreceptors in the Starburst cell. There are many experiments in the literature trying to prove that particular receptors work as autoreceptors (23–25). For the most part, these experiments try to investigate whether a cell containing a particular transmitter responds to that transmitter. It is known that Starburst cells respond to GABA, but no current or voltage responses to baclofen have been observed (39). However, we propose that baclofen has an effect on the muscarinic synapse without affecting particular conductances. An ideal experiment would measure baclofen's effect on ACh's release from Starburst cells synaptically isolated from the rest of the retina. One could attempt to isolate the Starburst cells synaptically by using low-Ca^{2+} media. Unfortunately, this condition would also shut down these cells' synapses, eliminating ACh release. Alternatively, one could use a cell culture to try to isolate the cholinergic Starburst cell. An experiment that is more feasible is to study whether the effect of baclofen on cholinergic and glycinergic releases is interrupted by drugs that interfere with G-protein pathways. This would not prove the existence of

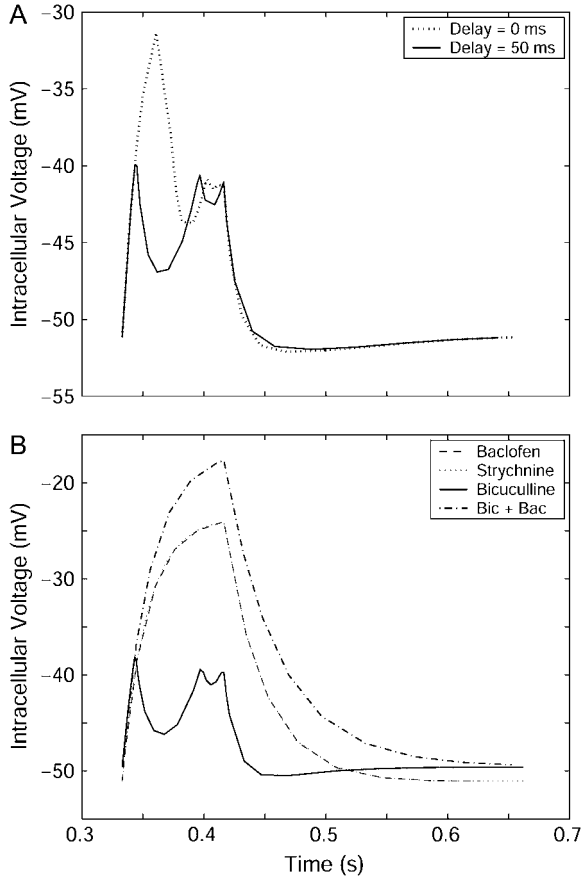

FIGURE 9 Effect of adding a constant delay to the $GABA_B$ synapse. We illustrate this effect by showing voltage at the right distal dendrite as in Fig. 2 *B*. Here, we show the results for a 50-ms delay. In panel *A*, we activate the bipolar cells sequentially to simulate motion. These cells are still activated by a 3-Hz square-wave (Eq. A1). However, the cycle of any given bipolar cell starts after that of the neighbor to its left by a preset delay. In this figure, this delay is 100 ms, implying an edge motion sweeping the Starburst cell in 400 ms from left to right. As predicted, the response to the motion is larger than the response to the full-field stimulation. In contrast, without the $GABA_B$ delay, motion facilitation over the full-field responses disappeared (see text for details). In panel *B*, we use full-field stimulation, with different combinations of drugs. The curves for baclofen and strychnine superimpose. Comparison of these curves with those in panel *A* reveals that even with the delay, these drugs augment the response. In turn, bicuculline on its own has little effect, but increases the effect of baclofen on the response ($Bic + Bac$), as in Figs. 7 and 8.

autoreceptors, but would provide circumstantial evidence for them as they tend to work through such proteins (30–32).

Another novel aspect of the model is that different types of GABAergic receptors may have different distributions across the Starburst cell's dendritic tree. Indirect evidence is now available for such different distributions of receptors (see Model for detailed arguments). The same differences should apply for cholinergic synapses. A test for such different distributions would be to use antibodies against these receptors and synapses in an identified Starburst cell. One could then check microscopically whether there are different distributions of immunoreactivity with the different antibodies. If such differences exist, then they would raise the possibility that the Starburst dendrite has more functionality than previously thought. Some studies propose that this cell's dendritic branches may function as independent electrotonic subunits (16,84,85,88). If different receptors and synapses have different distributions in the dendritic tree, then this may allow different portions of a dendritic branch to have different roles in information processing.

APPENDIX A: EQUATIONS

This Appendix presents all the equations used to simulate the model in Fig. 1.

Light stimuli

With the exception of the motion described in the Discussion, the light stimuli used in the simulations paralleled those used by Neal and Cunningham (5). Here, we will discuss the model only in the context of their stimuli. We used full-field square-wave stimulation,

$$S(t) = \begin{cases} a & \text{if } \dfrac{n}{f} \le t < \dfrac{n+d}{f}, n = 0, 1, 2, \ldots \\ 0 & \text{otherwise} \end{cases}, \qquad (1)$$

where a, f, and d are the amplitude, frequency, and duty-cycle of the wave, respectively.

Biophysical notation

Because the stimulus is full field, all the bipolar compartments in Fig. 1 respond alike. The same holds for the GABAergic compartments, glycinergic compartments, the two proximal dendritic compartments of the Starburst cell, and its two distal compartments. In this Appendix, we will denote a compartment by the subindex c. This subindex can attain the values of b, γ, g, s, p, and d for the bipolar, GABAergic, and glycinergic cells, soma of the Starburst cell, and its proximal and distal compartments, respectively. (Although the simulations do not include the ganglion cell, its subindex will be gc for simplifying the notation below.) Besides cells and compartments, release of neurotransmitters is identical for several different synapses containing the same transmitter. We will denote a neurotransmitter by the subindex n. This subindex can attain the values of gu for glutamate, γa for GABA released from GABAergic cells toward $GABA_A$ receptors, gy for glycine, γb for GABA released onto $GABA_B$ autoreceptors, and mu and ni for ACh released onto muscarinic and nicotinic receptors, respectively.

This article models the cellular compartments through standard cable-theory assumptions (89). The most important variable in this model is the compartment's potential (voltage), $V_c(t)$. A compartment's potential causes transmitter release, which is denoted by $R_{c_1,n,c_2}(t)$, with c_1 and c_2 being the pre- and postsynaptic compartments, respectively. For instance, $R_{p,\,mu,\,g}$ is the ACh release that activates muscarinic receptors from the proximal dendritic compartment of the Starburst cell onto the glycinergic cell. In turn, neurotransmitter release causes the activation of a membranous postsynaptic conductance, whose symbol is $g_{c_1,n,c_2}(t)$. Besides synaptic conductances, between any two neighbor compartments of the Starburst cell, there is an axial conductance g_{c_1,ax,c_2}. And all the model's compartments also have resting conductances, which we denote $g_{c,\,r,\,c}$.

We denote by $I_{x,y,c}$ the current flowing through the conductance $g_{x,y,c}$ into compartment c. To calculate this current, one needs the compartment's voltage ($V_c(t)$) and the conductance's reversal potential, $E_{y,c}$. The axial-conductance current flowing from compartment c_1 to compartment c is $I_{c_1,ax,c}$. From the axial and membranous currents, one can calculate the temporal evolution of the voltage at the compartment if one has its capacitance C_c. This capacitance and resting conductance were computed from the multiplication of the compartment's membranous area (A_c) by their specific values, denoted $\hat{C}$ and $\hat{g}_{r,c}$, respectively.

Synapses

All synapses in the model, except for the $GABA_B$ synapse, respond conventionally to presynaptic voltage. We model conventional synapses as if they are not the temporal bottlenecks of the system. The sigmoidal presynaptic-to-transmitter relationship in the model conventional synapses follows the steady-state input-output curves found experimentally (90,91). This relationship is

$$R_{c_1,n,c_2}(t) = \frac{\beta_{n,c_2}}{1 + \exp(-\alpha_n(V_c(t) - \theta_n))}, \qquad (2)$$

where $\beta_{n,c_2} > 0$ is the synapse's gain, $\alpha_n > 0$ is the slope of the synapse's input-output relationship, and θ_n is the synaptic threshold. Without loss of generality, one can set the post-synaptic conductance equals to release, since β_{n,c_2} could be made to have units of conductance:

$$g_{c_1,n,c_2}(t) = R_{c_1,n,c_2}(t). \qquad (3)$$

In Appendix B we express β_{n,c_2} with such units.

The $GABA_B$ synapse responds differently to presynaptic voltage than conventional synapses, since this synapse does not induce, directly, a conductance change (see Model). Instead, this synapse reduces the presynaptic Ca^{2+} conductance in the muscarinic synapse to the glycinergic cell. As a result, this synapse's gain falls. We model this fall by letting $\beta_{mu,\,g}$ depend on the locally released GABA,

$$\beta_{mu,g}(t) = \frac{\hat{\beta}_{mu,g}}{1 + R_{p,\gamma b,p}(t)}, \qquad (4)$$

where $\hat{\beta}_{mu,g} > 0$ is the gain of the muscarinic synapse when the $GABA_B$ receptors are not activated. (This equation assumes that the Starburst-cell release of GABA has the same dependence on presynaptic voltage as other releases (i.e., Eq. 2). This assumption cannot be, strictly speaking, correct. This is because we assume that this release is Ca^{2+} independent and thus not affected by the activation of the autoreceptors. The use of Eq. A2 is only justified for the sake of model simplicity, since there are no good models of Ca^{2+}-independent release.) Such a model must be taken as a simple abstraction of the complicated G-protein-dependent mechanism by which the $GABA_B$ autoreceptors work (30–32). A complete model would have to include the complete G-protein pathway.

Currents and potentials

This section describes how we calculate the voltages across the membranes of the different cellular compartments. This calculation is identical in all

compartments except for the bipolar cells. The currents flowing through synaptic or resting conductances depend on the voltage at nonbipolar compartments and on the conductances' reversal potentials. These currents are

$$I_{x,y,c}(t) = g_{x,y,c}(t)(E_{y,c} - V_c(t)). \quad (5)$$

The current flowing into compartment c from a compartment c_1 through an axial conductance is

$$I_{c_1,ax,c}(t) = g_{c_1,ax,c}(t)(V_{c_1}(t) - V_c(t)). \quad (6)$$

From these currents, the potential in the nonbipolar compartment follows

$$C_c \frac{dV_c(t)}{dt} = \sum_{i=1}^{N_c} I_{x_i,y_i,c}(t), \quad (7)$$

where N_c is the number of types of currents flowing into compartment c.

The bipolar cells are special cases among all compartments, because one of its inputs does not come from synapses but directly from light. We model this input as a current being injected onto the bipolar compartment. In addition, this compartment receives a GABAergic current and has a resting-conductance current (Fig. 1), making $N_b = 3$ in Eq. A7. For simplicity, the stimulus current is exactly $S(t)$ (Eq. A1). This means that the simulations neglect the temporal properties of the photoreceptors feeding the bipolar cells, that is, they consider the input's dynamic sufficiently slow. For the same reason, the simulations assume that the bipolar compartment has zero capacitance, that is, $C_b = 0$. With these assumptions, one can set the left-hand side of Eq. A7 to 0 and use Eq. A5 to get

$$V_b(t) = \frac{S(t) + g_{b,r,b}E_{r,b} + g_{\gamma,\gamma a,b}(t)E_{\gamma a,b}}{g_{b,r,b} + g_{\gamma,\gamma a,b}(t)},$$

where $g_{\gamma,\ \gamma a,\ b}(t)$ obeys Eq. 3. This voltage is then fed to the bipolar synapse, whose glutamatergic release is governed by Eq. 2.

APPENDIX B: PARAMETERS

This Appendix presents the simulation parameters, with the notation of Appendix A, and organized in four sets: stimulus, synaptic, cellular, and pharmacology.

Stimulus parameters

The three parameters of the stimulus (Eq. 1) were $a = 8$ pA, $f = 3$ Hz, and $d = 0.25$.

Synaptic parameters

We present the synaptic parameters (Eqs. 2–5) in six subsets: glutamatergic, $GABA_A$, glycinergic, $GABA_B$, muscarinic, and nicotinic synapses.

Glutamatergic synapses

$$\alpha_{gu} = 0.5\,\mathrm{mV}^{-1};\ \theta_{gu} = -40\,\mathrm{mV};\ \beta_{gu,g} = \beta_{gu,s} = \beta_{gu,p} = \beta_{gu,d} = 50\,\mathrm{pS};\ E_{gu,g} = E_{gu,s} = E_{gu,p} = E_{gu,d} = 20\,\mathrm{mV}.$$

$GABA_A$ synapses

$$\alpha_{\gamma a} = 1\,\mathrm{mV}^{-1};\ \theta_{\gamma a} = -50\,\mathrm{mV};\ \beta_{\gamma a,b} = 200\,\mathrm{pS};\ \beta_{\gamma a,d} = 25\,\mathrm{pS};\ E_{\gamma a,b} = -50\,\mathrm{mV};\ E_{\gamma a,d} = -60\,\mathrm{mV}.$$

Glycinergic synapses

$$\alpha_{gy} = 1\,\mathrm{mV}^{-1};\ \theta_{gy} = -40\,\mathrm{mV};\ \beta_{gy,s} = \beta_{gy,p} = \beta_{gy,d} = 250\,\mathrm{pS};\ E_{gy,s} = E_{gy,p} = E_{gy,d} = -60\,\mathrm{mV}.$$

$GABA_B$ synapses

$$\alpha_{\gamma b} = 1\,\mathrm{mV}^{-1};\ \theta_{\gamma b} = -40\,\mathrm{mV};\ \beta_{\gamma b,p} = 25\,\mathrm{pS}.$$

Muscarinic synapses

$$\alpha_{mu} = 10\,\mathrm{mV}^{-1};\ \theta_{mu} = -40\,\mathrm{mV};$$
$$\hat{\beta}_{mu,g} = 250\,\mathrm{pS};\ E_{mu,g} = 0\,\mathrm{mV}.$$

Nicotinic synapses

$$\alpha_{ni} = 0.312\,\mathrm{mV}^{-1};\ \theta_{ni} = -46\,\mathrm{mV};\ \beta_{ni,gc} = 250\,\mathrm{pS}.$$

The only exception is that $\hat{\beta}_{mu,g} = 125$ pS for the central glycinergic cell, so its total muscarinic input is equal to the other glycinergic cells in the full-field experiments.

Cellular parameters

Three cellular parameters (Eqs. 5–7) were identical for all compartments: the specific membrane capacitance ($\hat{C} = 1\ \mu\mathrm{F/cm}^2$), the resting potential ($E_{r,c} = -50$ mV), and the axial conductance ($g_{c_1,ax,c_2} = 50$ pS). The rest of parameters are organized in two sets: compartmental membranous areas and specific resting conductances.

Compartmental membranous areas

$$A_b = A_\gamma = A_s = 1000\,\mu\mathrm{m}^2;\ A_g = A_p = A_d = 250\,\mu\mathrm{m}^2.$$

Specific resting conductances

$$\hat{g}_{r,b} = \hat{g}_{r,\gamma} = \hat{g}_{r,s} = \hat{g}_{r,p} = \hat{g}_{r,d} = 20\,\mu\mathrm{S/cm}^2;\ \hat{g}_{r,g} = 10\,\mu\mathrm{S/cm}^2.$$

Pharmacology parameters

The simulations of the pharmacology were performed by setting the appropriate parameters to zero when a particular drug was used. We present the pharmacology parameters in three subsets: baclofen, strychnine, and bicuculline.

Baclofen

$$\hat{\beta}_{mu,g} = 0.$$

Strychnine

$$\beta_{gy,s} = \beta_{gy,p} = \beta_{gy,d} = 0.$$

Bicuculline

$$\beta_{\gamma a,\,d} = 0.$$

We thank Susmita Chatterjee, Eun-Jin Lee, David Merwine, Mónica Padilla, Joaquín Rapela, and Jeff Wurfel for discussions during the performance of this project. We also thank Ms. Denise Steiner for administrative help.

This work was supported by National Eye Institute grants No. EY08921 and No. EY11170 to N.M.G., and by National Eye Institute grant No. EY07552 to C.L.Z.

REFERENCES

1. Brecha, N., D. Johnson, L. Peichl, and H. Wässle. 1988. Cholinergic amacrine cells of the rabbit retina contain glutamate decarboxylase and γ-aminobutyrate immunoreactivity. *Proc. Natl. Acad. Sci. USA.* 85: 6187–6191.
2. Kosaka, T., M. Tauchi, and J. L. Dahl. 1988. Cholinergic neurons containing GABA-like and/or glutamic acid decarboxylase-like immunoreactivities in various brain regions of the rat. *Exp. Brain Res.* 70: 605–617.
3. Nguyen, L. T., and N. M. Grzywacz. 2000. Co-localization of choline acetyltransferase and GABA in the developing and adult turtle retinas. *J. Comp. Neurol.* 420:527–538.
4. Vaney, D. I., and H. M. Young. 1988. GABA-like immunoreactivity in cholinergic amacrine cells of the rabbit retina. *Brain Res.* 438:369–373.
5. Neal, M. J., and J. R. Cunningham. 1995. Baclofen enhancement of acetylcholine release from amacrine cells in the rabbit retina by reduction of glycinergic inhibition. *J. Physiol. (Lond.).* 482:363–372.
6. Fried, S. I., T. A. Munch, and F. S. Werblin. 2002. Mechanisms and circuitry underlying directional selectivity in the retina. *Nature.* 420: 411–414.
7. Fried, S. I., T. A. Munch, and F. S. Werblin. 2005. Directional selectivity is formed at multiple levels by laterally offset inhibition in the rabbit retina. *Neuron.* 46:117–127.
8. Massey, S. C., D. M. Linn, C. A. Kittila, and W. Mirza. 1997. Contributions of $GABA_A$ receptors and $GABA_C$ receptors to acetylcholine release and directional selectivity in the rabbit retina. *Vis. Neurosci.* 14:939–948.
9. O'Malley, D. M., and R. H. Masland. 1993. Responses of the Starburst amacrine cells to moving stimuli. *J. Neurophysiol.* 69:730–738.
10. Amthor, F. R., N. M. Grzywacz, and D. K. Merwine. 1996. Extra-receptive field facilitation in On-Off DS ganglion cells of the rabbit retina. *Vis. Neurosci.* 13:303–310.
11. Masland, R. H., W. Mills, and C. Cassidy. 1984. The functions of acetylcholine in the rabbit retina. *Proc. R. Soc. Lond. B Biol. Sci.* 223: 121–139.
12. Schmidt, M., M. Humphrey, and H. Wässle. 1987. Action and localization of acetylcholine in the cat retina. *Neurosci. Lett.* 59:235–240.
13. Amthor, F. R., K. T. Keyser, and N. A. Dmitrieva. 2002. Effects of the destruction of Starburst-cholinergic amacrine cells by the toxin AF64A on rabbit retinal directional selectivity. *Vis. Neurosci.* 19:495–509.
14. Ariel, M., and A. R. Adolph. 1985. Neurotransmitter inputs to directionally sensitive turtle retinal ganglion cells. *J. Neurophysiol.* 54: 1123–1143.
15. Ariel, M., and N. W. Daw. 1982a. Pharmacological analysis of directionally sensitive rabbit retinal ganglion cells. *J. Physiol. (Lond.).* 324:161–185.
16. Grzywacz, N. M., J. S. Tootle, and F. R. Amthor. 1997. Is the input to a GABAergic or cholinergic synapse the sole asymmetry in rabbit's retinal directional selectivity? *Vis. Neurosci.* 14:39–54.
17. Grzywacz, N. M., F. R. Amthor, and D. K. Merwine. 1998. Necessity of ACh for retinal directionally selective responses to drifting gratings in rabbit. *J. Physiol. (Lond.).* 512:575–581.
18. Kittila, C. A., and S. C. Massey. 1997. Pharmacology of directionally selective ganglion cells in the rabbit retina. *J. Neurophysiol.* 77: 675–689.
19. Reed, B. T., K. T. Keyser, and F. R. Amthor. 2004. MLA-sensitive cholinergic receptors involved in the detection of complex moving stimuli in retina. *Vis. Neurosci.* 21:861–872.
20. Yoshida, K., D. Watanabe, H. Ishikane, M. Tachibana, I. Pastan, and S. Nakanishi. 2001. A key role of Starburst amacrine cells in originating retinal directional selectivity and optokinetic eye movement. *Neuron.* 30:771–780.
21. Gavrikov, K. E., A. V. Dmitriev, K. T. Keyser, and S. C. Mangel. 2003. Cation-chloride cotransporters mediate neural computation in the retina. *Proc. Natl. Acad. Sci. USA.* 100:16047–16052.
22. Zucker, C. L., J. E. Nilson, B. Ehinger, and N. M. Grzywacz. 2005. Compartmental localization of $GABA_B$ receptors in the cholinergic circuitry of the rabbit retina. *J. Comp. Neurol.* 493:448–459.
23. Anderson, R. A., and R. Mitchell. 1985. Evidence of $GABA_B$ autoreceptors in median eminence. *Eur. J. Pharmacol.* 118:355–358.
24. Langer, S. Z. 1997. 25 years since the discovery of presynaptic receptors: present knowledge and future perspectives. *Trends Pharmacol. Sci.* 18:95–99.
25. Phelan, K. D. 1999. *N*-Ethylmaleimide selectively blocks presynaptic $GABA_B$ autoreceptor but not heteroreceptor-mediated inhibition in adult rat striatal slices. *Brain Res.* 847:308–313.
26. Hirsch, J. C., and Y. Burnod. 1987. A synaptically evoked late hyperpolarization in the rat dorsolateral geniculate neurons in vitro. *Neuroscience.* 23:457–468.
27. Yamada, K., B. Yu, and J. P. Gallagher. 1999. Different subtypes of $GABA_B$ receptors are present at pre- and postsynaptic sites within the rat dorsolateral septal nucleus. *J. Neurophysiol.* 81:2875–2883.
28. Bindokas, V. P., and A. T. Ishida. 1991. (−)-Baclofen and γ-aminobutyric acid inhibit calcium currents in isolated retinal ganglion cells. *Proc. Natl. Acad. Sci. USA.* 88:10759–10763.
29. Heidelberger, R., and G. Matthews. 1991. Inhibition of calcium influx and calcium current by γ-aminobutyric acid in single synaptic terminals. *Proc. Natl. Acad. Sci. USA.* 88:7135–7139.
30. Maguire, G., B. Maple, P. Lukasiewicz, and F. Werblin. 1989. Gamma-aminobutyrate type-B receptor modulation of L-type calcium channel current at bipolar cell terminals in the retina of the tiger salamander. *Proc. Natl. Acad. Sci. USA.* 86:10144–10147.
31. Brody, D. L., and D. T. Yue. 2000. Relief of G-protein inhibition of calcium channels and short-term synaptic facilitation in cultured hippocampal neurons. *J. Neurosci.* 20:889–898.
32. Dolphin, A. C., and R. H. Scott. 1986. Inhibition of calcium currents in cultured rat dorsal root ganglion neurones by (−)-baclofen. *Br. J. Pharmacol.* 88:213–220.
33. Shen, W., and M. M. Slaughter. 1999. Metabotropic GABA receptors facilitate L-type and inhibit N-type calcium channels in single salamander retinal neurons. *J. Physiol. (Lond.).* 516:711–718.
34. Koulen, P., B. Malitschek, R. Kuhn, B. Bettler, H. Wässle, and J. H. Brandstatter. 1998. Presynaptic and postsynaptic localization of $GABA_B$ receptors in neurons of the rat retina. *Eur. J. Neurosci.* 10:1446–1456.
35. Wright, L. L., C. L. Macqueen, G. N. Elston, H. M. Young, D. V. Pow, and D. I. Vaney. 1997. The DAPI-3 amacrines cells of the rabbit retina. *Vis. Neurosci.* 14:473–492.
36. Zucker, C. L., and B. Ehinger. 1998. Gamma-aminobutyric acid receptors on a bistratified amacrine cell type in the rabbit retina. *J. Comp. Neurol.* 393:309–319.
37. Zucker, C. L., and B. Ehinger. 2001. Complexities of retinal circuitry revealed by neurotransmitter receptor localization. *Prog. Brain Res.* 131:71–81.
38. Wasselius, J., K. Johansson, A. Bruun, C. Zucker, and B. Ehinger. 1998. Correlations between cholinergic neurons and muscarinic m2 receptors in the rat retina. *Neuroreport.* 9:1799–1802.
39. Zhou, Z. J., and G. L. Fain. 1995. Neurotransmitter receptors of Starburst amacrine cells in rabbit retina slices. *J. Neurosci.* 15:5334–5345.

40. Brandstatter, J. H., U. Greferath, T. Euler, and H. Wässle. 1995. Co-stratification of $GABA_A$ receptors with the directionally selective circuitry of the rat retina. *Vis. Neurosci.* 12:345–358.
41. Zucker, C. L., B. Ehinger, and N. M. Grzywacz. 1998. $GABA_B$ receptors are localized to Starburst amacrine and ganglion cells in the rabbit retina. *Soc. Neurosci. Abstr.* 24:136.
42. Amthor, F. R., C. W. Oyster, and E. S. Takahashi. 1984. Morphology of ON-OFF direction-selective ganglion cells in the rabbit retina. *Brain Res.* 298:187–190.
43. Amthor, F. R., E. S. Takahashi, and C. W. Oyster. 1989. Morphologies of rabbit retinal ganglion cells with complex receptive fields. *J. Comp. Neurol.* 280:97–121.
44. Famiglietti, E. V., Jr. 1983. Starburst amacrine cells and cholinergic neurons: mirror-symmetric on and off amacrine cells of rabbit retina. *Brain Res.* 261:138–144.
45. Nelson, R., E. V. Famiglietti, and H. Kolb. 1978. Intracellular staining reveals different levels of stratification for on- and off-center ganglion cells in cat retina. *J. Neurophysiol.* 41:472–483.
46. Tauchi, M., and R. H. Masland. 1984. The shape and arrangement of the cholinergic neurons in the rabbit retina. *Proc. R. Soc. Lond. B Biol. Sci.* 223:101–119.
47. Ozaita, A., J. Petit-Jacques, B. Volgyi, C. S. Ho, R. H. Joho, S. A. Bloomfield, and B. Rudy. 2004. A unique role for K_v3 voltage-gated potassium channels in Starburst amacrine cell signaling in mouse retina. *J. Neurosci.* 24:9335–9343.
48. Hofmann, H. D., and V. Mockel. 1991. Release of γ-amino[3H]butyric acid from cultured amacrine-like neurons mediated by different excitatory amino acid receptors. *J. Neurochem.* 56:923–932.
49. Lopez-Costa, J. J., J. Goldstein, J. Pecci-Saavedra, V. M. Della Maggiore, M. A. De Las Heras, M. I. Sarmiento, and R. E. Rosenstein. 1999. GABA release mechanism in the golden hamster retina. *Int. J. Neurosci.* 98:13–25.
50. Schwartz, E. A. 1982. Calcium-independent release of GABA from isolated horizontal cells of the toad retina. *J. Physiol. (Lond.).* 323:211–227.
51. Zheng, J. J., S. Lee, and Z. J. Zhou. 2004. A developmental switch in the excitability and function of the Starburst network in the mammalian retina. *Neuron.* 44:851–864.
52. Ariel, M., and N. W. Daw. 1982. Effects of cholinergic drugs on receptive field properties of rabbit retinal ganglion cells. *J. Physiol. (Lond.).* 324:135–160.
53. Brandon, C. 1987. Cholinergic neurons in the rabbit retina: dendritic branching and ultrastructural connectivity. *Brain Res.* 426:119–130.
54. Famiglietti, E. V., Jr. 1991. Synaptic organization of Starburst amacrine cells in rabbit retina: analysis of serial thin sections by electron microscopy and graphic reconstruction. *J. Comp. Neurol.* 309:40–70.
55. Masland, R. H., and A. Ames III. 1976. Responses to acetylcholine of ganglion cells in an isolated mammalian retina. *J. Neurophysiol.* 39: 1220–1235.
56. Yazejian, B., and G. L. Fain. 1993. Whole-cell currents activated at nicotinic acetylcholine receptors on ganglion cells isolated from goldfish retina. *Neuroreport.* 9:1799–1802.
57. Linn, D. M., and S. C. Massey. 1992. GABA inhibits ACh release from the rabbit retina: a direct effect or feedback to bipolar cells? *Vis. Neurosci.* 8:97–106.
58. Gillette, M. A., and R. F. Dacheux. 1995. GABA- and glycine-activated currents in the rod bipolar cell of the rabbit retina. *J. Neurophysiol.* 74:856–875.
59. Qian, H., and J. E. Dowling. 1995. $GABA_A$ and $GABA_C$ receptors on hybrid bass retinal bipolar cells. *J. Neurophysiol.* 74:1920–1928.
60. Suzuki, S., M. Tachibana, and A. Kaneko. 1990. Effects of glycine and GABA on isolated bipolar cells of the mouse retina. *J. Physiol. (Lond.).* 421:645–662.
61. Thoreson, W. B., and R. F. Miller. 1993. *J. Neurophysiol.* 70:1326–1338.
62. Feigespan, A., H. Wässle, and J. Bormann. 1993. Pharmacology of GABA receptor Cl^- channels in rat retinal bipolar cells. *Nature.* 361:159–162.
63. Lukasiewicz, P. D., and F. S. Werblin. 1994. A novel GABA receptor modulates synaptic transmission from bipolar to ganglion and amacrine cells in the tiger salamander retina. *J. Neurosci.* 14:1213–1223.
64. Matthews, G., G. S. Ayoub, and R. Heidelberger. 1994. Presynaptic inhibition of GABA is mediated via two distinct GABA receptors with novel pharmacology. *J. Neurosci.* 14:1079–1090.
65. Dormand, J. R., and P. J. Prince. 1980. A family of embedded Runge-Kutta formulae. *J. Compar. Applied Math.* 6:19–26.
66. Coleman, P. A., and R. F. Miller. 1989. Measurement of passive membrane parameters with whole-cell recording from neurons in the intact amphibian retina. *J. Neurophysiol.* 61:218–230.
67. Johnston, D., and T. H. Brown. 1983. Interpretation of voltage-clamp measurements in hippocampal neurons. *J. Neurophysiol.* 50: 464–486.
68. Redman, S., and B. Walmsley. 1983. The time course of synaptic potentials evoked in cat spinal motoneurones at identified group IA synapses. *J. Physiol. (Lond.).* 343:117–133.
69. Stafstrom, C. E., P. C. Schwindt, and W. E. Crill. 1984. Cable properties of layer V neurons from cat sensorimotor cortex in vitro. *J. Neurophysiol.* 52:278–289.
70. Marchiafava, P.L., and V Torre. 1978. The responses of amacrine cells to light and intracellularly applied currents. *J. Physiol. (Lond.).* 276:83–102.
71. Nelson, R. 1982. AII amacrine cells quicken time course of rod signals in the cat retina. *J. Neurophysiol.* 47:928–947.
72. Rodieck, R. W. 1989. Starburst amacrine cells of the primate retina. *J. Comp. Neurol.* 285:18–37.
73. Hayes, B. P. 1984. Cell populations of the ganglion cell layer: displaced amacrine and matching amacrine cells in the pigeon retina. *Exp. Brain Res.* 56:565–573.
74. Kaneko, A., and M. Tachibana. 1986. Effects of γ-aminobutyric acid on isolated cone photoreceptors of the turtle retina. *J. Physiol. (Lond.).* 373:443–461.
75. Barnes, S., and F. Werblin. 1987. Direct excitatory and lateral inhibitory synaptic inputs to amacrine cells in the tiger salamander retina. *Brain Res.* 406:233–237.
76. Jones, S. W. 1987. A muscarine-resistant M-current in C cells of bullfrog sympathetic ganglia. *Neurosci. Lett.* 74:309–314.
77. Zholos, A. V., and T. B. Bolton. 1995. Effects of divalent cations on muscarinic receptor cationic current in smooth muscle from Guinea-pig small intestine. *J. Physiol. (Lond.).* 486:67–82.
78. Takai, Y., R. Sugawara, H. Ohinata, and A. Takai. 2004. Two types of non-selective cation channel opened by muscarinic stimulation with carbachol in bovine ciliary muscle cells. *J. Physiol. (Lond.).* 559: 899–922.
79. Sanchez, R., and C. S. Leonard. 1996. NMDA-receptor-mediated synaptic currents in Guinea pig laterodorsal tegmental neurons in vitro. *J. Neurophysiol.* 76:1101–1111.
80. Nelder, J. A., and R. Mead. 1965. A Simplex method for function minimization. *Computer J.* 7:308–313.
81. Dong, C. J., and F. S. Werblin. 1998. Temporal contrast enhancement via $GABA_C$ feedback at bipolar terminals in the tiger salamander. *J. Neurophysiol.* 79:2171–2180.
82. Werblin, F., G. Maguire, P. Lukasiewicz, S. Eliasof, and S. M. Wu. 1988. Neural interactions mediating the detection of motion in the retina of the tiger salamander. *Vis. Neurosci.* 1:317–329.
83. Zhang, J., C. S. Jung, and M. M. Slaughter. 1997. Serial inhibitory synapses in the retina. *Vis. Neurosci.* 14:553–563.
84. Borg-Graham, L. J., and N. M. Grzywacz. 1991. A model of the direction selectivity circuit in retina: transformations by neurons singly and in concert. *In* Single Neuron Computation. T. McKenna, J. Davis, and S. F. Zornetzer, editors. Academic Press, Orlando, FL. 347–375.
85. Euler, T., P. B. Detwiler, and W. Denk. 2002. Directionally selective calcium signals in dendrites of Starburst amacrine cells. *Nature.* 418: 845–852.

86. Barlow, H. B., and W. R. Levick. 1965. The mechanism of directionally selective units in the rabbit's retina. *J. Physiol. (Lond.).* 178: 477–504.

87. Grzywacz, N. M., and F. R. Amthor. 1993. Facilitation in on-off directionally selective ganglion cells in the rabbit retina. *J. Neurophysiol.* 69:2188–2199.

88. Tukker, J. J., W. R. Taylor, and R. G. Smith. 2004. Direction selectivity in a model of the Starburst amacrine cell. *Vis. Neurosci.* 21:611–625.

89. Rall, W., R. E. Burke, W. R. Holmes, J. J. Jack, S. J. Redman, and I. Segev. 1992. Matching dendritic neuron models to experimental data. *Physiol. Rev.* 72:S159–S186.

90. Katz, B., and R. Miledi. 1967. A study of synaptic transmission in the absence of nerve impulses. *J. Physiol. (Lond.).* 192:406–436.

91. Kusano, K. 1970. Influence of ionic environment on the relationship between pre- and postsynaptic potentials. *J. Neurobiol.* 1: 435–457.